

A novel method of reducing melting temperatures in SnAg and SnCu solder alloys

Rami N. Chukka · Suresh Telu · Bhargava NRMR ·
Lang Chen

Received: 15 February 2010 / Accepted: 29 April 2010 / Published online: 14 May 2010
© Springer Science+Business Media, LLC 2010

Abstract With the increasing use of lead-free solder alloys in modern electronics, low melting materials are often required to protect the heat-sensitive parts during soldering operation. Alloy systems based on Sn/Cu/Ag offer more reliable solutions and address the current problems involved with soldering process. Nanoparticles melt relatively at low temperatures compared to their bulk counter parts and we introduce a robust method of synthesizing nanoscale solder pastes for wave soldering applications. Nanoparticles of Sn-3.5Ag and Sn-0.7Cu alloys were prepared with stir casting followed by mechanical attrition. The size dependent melting properties of the eutectic alloys were studied by differential scanning calorimetry technique and the results showed a reduction of 4.7 and 5.0 °C melting temperatures in the alloys when reduced from bulk to 92 nm and 96 nm sizes respectively. The nanosize effects were also theoretically calculated and compared with experimental data.

1 Introduction

Environmental regulations demands the solder materials for electronic components and printed wiring board interconnections must be lead-free. Lead-free solder alloys such as Sn/Ag/Cu based systems become increasingly popular as reliable substitutions to Pb based solders. However, they generally have liquidus points of 220 °C or higher,

compared to the 183 °C melting point of conventional tin–lead solders. The high melting point alloys require higher processing temperatures, with reflow process temperatures typically above 240 °C. The high reflow temperatures can cause damages to the printed boards and results in low mechanical stability. The European program on Improved Design life and Environmental Assemblies by Lead-free Soldering, (IDEALS) recommended the ternary Sn-3.8Ag-0.7Cu as a possible replacement to lead containing alloys in reflow applications [1]. Subsequently, the National Electronics Manufacturing Initiative (NEMI) chose the Sn-3.9Ag-0.6Cu for surface mount applications and the Sn-0.7Cu as the first choice, and the Sn-3.5Ag as the second for wave soldering applications [2].

Many materials, including pure metals, exhibit a change in properties as their particle sizes approach nanoscale dimensions. The increase in the surface-to-volume ratio, which occurs naturally as particle sizes shrink, necessarily increases the relative proportion of higher energy surface atoms. The effect may include a change in reactivity, change in electromagnetic properties, altering electronic and optical properties [3]. Takagi first observed melting point depression of several types of metal nanoparticles in 1954 [4]. A variable intensity electron beam from a transmission electron microscope was used to melt metal nanoparticles in early experiments. Diffraction patterns changed from characteristic crystalline patterns to liquid patterns as the small particles melted, allowing Takagi to estimate the melting temperature from the electron beam energy. The phenomenon of melting point depression of nanoscale metal particles has been extensively studied after 1960s, when it was noticed that extremely thin evaporated particles of metal have a lower melting point than the bulk material. Evaporated tin particles and gold nano-scale particles were studied by Buffat and Borel, who

R. N. Chukka (✉) · S. Telu · B. NRMR
Department of Metallurgical Engineering, Andhra University,
Visakhapatnam 530003, India
e-mail: rami0002@ntu.edu.sg

R. N. Chukka · L. Chen
School of Materials Science and Engineering, Nanyang
Technological University, Singapore 639798, Singapore

demonstrated melting point depressions of well over 50% compared to the bulk melting point of gold [3].

In this work, we investigated the size dependence of melting properties of tin-rich alloys for soldering applications. Eutectic compositions of Sn-3.5Ag and Sn-0.7Cu alloys are identified from literature as alternatives to lead-based solder alloy due to their excellent physical and mechanical characteristics [2, 5]. Experimental investigations were carried out in the direction of cutting down the melting temperature of the proposed alloys as close to the eutectic tin–lead alloy. The change in melting temperature (T_m) with particle size is a surface initiated process [6, 7] and we employed mechanical attrition process to produce nano particles & tested for melting properties. We showed a maximum melting temperature reduction of 5.0 °C in Sn-0.7Cu system and 4.7 °C in Sn-3.5 Ag system at average particle sizes of 96 nm and 92 nm respectively. Also a theoretical model has been proposed to predict further size dependent lowering of T_m of small particles, and the results were compared with the experimental data.

2 Experimental

2.1 Alloy preparation

Eutectic alloys were prepared by conventional stir-cast technique from stoichiometric amounts of individual metals melted separately under protective environments and later mixed in a graphite crucible while stirring. The molten mixtures were maintained slightly at higher temperatures than required for melting to prevent immediate solidification during casting due to heat losses while mixing. The alloys were cast into a metallic mold by ensuring uniform mixing by mechanical agitation. For instance, to prepare a ~310 gm of binary alloy of Sn-3.5 Ag, 300 gm of Sn and 10.5 gm of Ag were weighed separately to prepare the stoichiometric composition. A mixture of 100 gm of Sn and 10.5 gm of Ag was initially heated up in a furnace which is operated at 900 °C for 50 min. While doing so, the copper completely get melted and form solid solution with tin. Once the solid solution is formed, it will be stable after even at lower temperatures. Then pure Sn of weight 200 gm was added to the molten alloy and placed in a furnace at 250 °C for 60 min to make sure complete melting of Sn. This process ensures minimum overheating of the liquid solution and there by less oxidation at high temperatures. To prevent the oxidation of molten solution, coverall powder is added in a ratio of 1000:1. The Molten mixture was then cast in a metallic mould and later the cast structure machined into small chips on Lathe in order to accommodate them in high energy ball mill for further size reduction.

2.2 Synthesis of nanopowders

Unlike the chemical reduction methods, mechanical milling is simple and robust technique for mass production of nanoparticles. The solid-state process technique produces particles with submicron homogeneity by repeated welding, fracturing, and rewelding of powder particles. It is convenient to use the method to produce commercial solder pastes by adding flux directly to powders. Nanopowders of the binary alloys were prepared by using high energy ball milling route. Milling was performed at room temperature and the ball-to-powder weight ratio was maintained at 20:1 throughout the process. The rotation speed was fixed at 150 rpm for both dry and wet milling conditions. Wet milling was carried in toluene medium to avoid the cold welding of particles once the size reached to below 200 nm. We limited the total milling time of the attrition process to 50 h and after that no further reduction in size of the particles were observed. First 20 h of milling was carried in dry mode and next 30 h of grinding conducted in liquid medium. Representative samples were collected after every 10 h of grinding process and preserved them in toluene medium. The recrystallization temperatures of the eutectic alloys chosen for this study are showing their values lie below room temperature. Under these circumstances, the stored energies due to the residual stresses during the milling process are annihilated by recovery and recrystallization mechanisms at ambient temperature.

2.3 Characterization

The powder samples were analyzed by using X-ray diffractometer [(D/MAX-B, Rigaku); Cu $K\alpha$, $\lambda = 1.5406 \text{ \AA}$] to estimate crystallite size and to identify the phases present in. The crystallite sizes were calculated from peak broadening values by using Scherrer's equation. In parallel, thermometric studies of the alloys were performed by using differential scanning calorimeter (DSC), with a Pyris 1, using Argon atmosphere and a ramp rate of 10 °C per minute used for both Sn-3.5Ag and Sn-0.7Cu alloys. Onset calculations used to determine the difference in melting temperatures of the eutectic alloys and temperature range used for measurements are 175–275 °C.

3 Results & discussions

Nanopowders of as-synthesized binary alloys were prepared by high energy ball milling technique and the size reduction trends were plotted against milling times (in Fig. 1). The size of the particles were quickly reduced from bulk to ~300 nm in first 10 h of milling and thereafter the reduction was sluggish. This is because of the alloys are

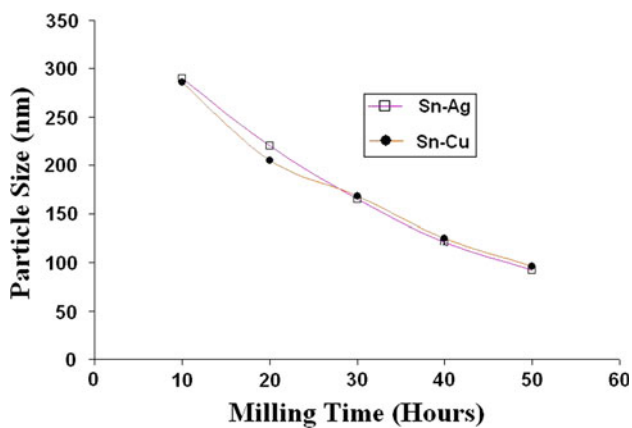
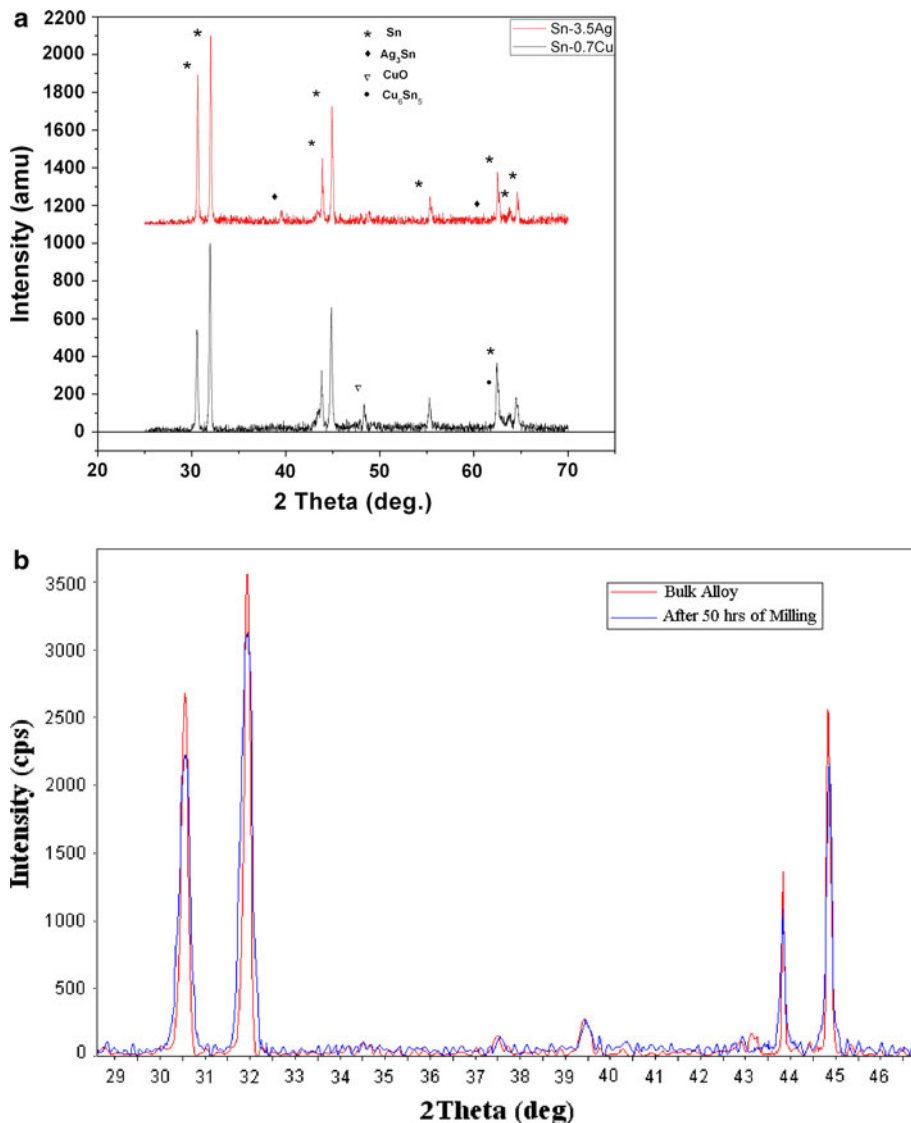


Fig. 1 Variation of particle size of the binary alloys with milling time

highly ductile at ambient conditions and it leads repeated cold welding of particles as the sizes reaches down to several nanometers. The reduction rates were further

Fig. 2 a X-Ray diffraction patterns of bulk eutectic alloys
b peak broadening due to size effects



getting reduced even in wet milling process and the slope of the curves become linear at higher milling times. After 50 h of milling, the final sizes of the particles found to be 92 and 96 nm in Sn-3.5Ag and Sn-0.7Cu systems.

3.1 Structural analysis

The XRD patterns of bulk alloys are shown in Fig. 2a. The diffraction pattern of Sn-3.5 Ag alloy indexed with a majority of β -Sn phase and the Ag_3Sn phase, implying successful alloying of Sn and Ag during casting process. No prominent oxide peak was observed in the diffraction measurements. The Sn, and Cu_6Sn_5 phases were detected along with a weak oxide peak from CuO phase in Sn-0.7Cu system, indicating that copper partially oxidized during melting process at high temperatures. The amount of the flux powder added is still insufficient to protect it from oxidation.

A representative plot of Sn-3.5Ag alloy was shown in Fig. 2b to depict the peak broadening in Cu-3.5Ag alloy from bulk to 50 h of milled sample. The breadth of the real line profile (B) is inversely proportional to the size (Z) of the coherently diffracting domains in a direction perpendicular to the diffracting planes according to Scherrer's equation; ($Z = 0.891\lambda/(B \cos \theta)$). Broadening of peaks attributed to continuous size reduction of the powders during milling. The other possibility of peak broadening from residual stresses during milling process was double checked by annealing the powder samples at 60 °C (to make sure the annealing temperatures are well above recrystallization temperatures of both the alloys) under 10^{-6} Pa vacuum for 1 h period. There were no changes observed in peak broadening values before and after annealing process. This confirms that the samples are obtained in stress free state after the milling process.

3.2 Melting properties

The melting properties of the bulk and powder samples were analyzed by DSC and the results are shown below. Figure 3 shows single endothermic peaks corresponding to the melting of the eutectic alloys during heating at rate of 10 °C/min. The melting points of the alloys are derived from the corresponding melting peaks and shown in the figure. The melting temperature of Sn-Cu alloy found to be slightly higher compared to literature value. This might be due to the partial oxidation of copper cause in loss of copper, which shifts the alloy composition to left hand side from eutectic composition in Sn-Cu phase diagram and also CuO increases the melting value.

Sharp endothermic peaks observed at 223.5 and 228.3 °C in bulk Sn3.5Ag and Sn0.7Cu alloys and as the milling time increases, the peaks gradually broadened and shifted to lower temperatures side. This clearly indicates that the surface effects contributed in lowering the melting temperatures due to the decrease of crystallite sizes, as observed in the work of Buffat and Borel [3]. The differences in melting temperatures of bulk and nanosized materials were found to be 4.7 and 5.0 °C in tin-silver and tin-copper systems respectively. After first cycle of melting and cooling processes, the melting temperature changes were observed to be 0.31 and 0.24 °C in both the alloys.

3.3 Theoretical predictions

The melting point depression due to nanosize effects were calculated theoretically for Sn-3.5Ag and Sn-0.7Cu alloys as a function of nanoparticle size, since it is believed that the melting point depression phenomenon also occurs for eutectic alloys in similar way as for pure metals. The

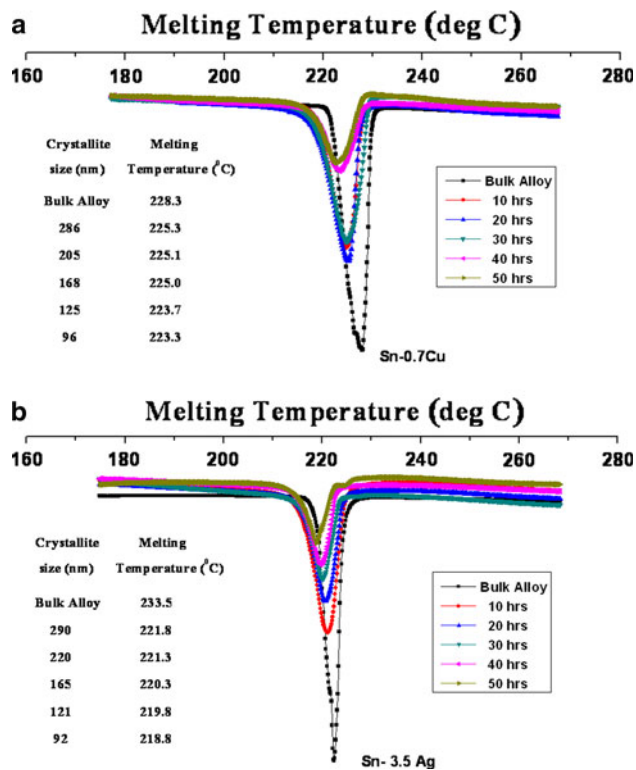


Fig. 3 DSC curves of **a** Sn-0.7Cu and **b** Sn-3.5Ag cast alloys and nanoparticles

calculations were carried out by using the following model [3, 8]:

$$\Delta T = T_m^{\text{bulk}} - T_m(r) = \frac{T_m^{\text{bulk}}}{H_m^{\text{bulk}} \rho_S r} \left(\sigma_S - \sigma_L \left(\frac{\rho_S}{\rho_L} \right)^{\frac{2}{3}} \right)$$

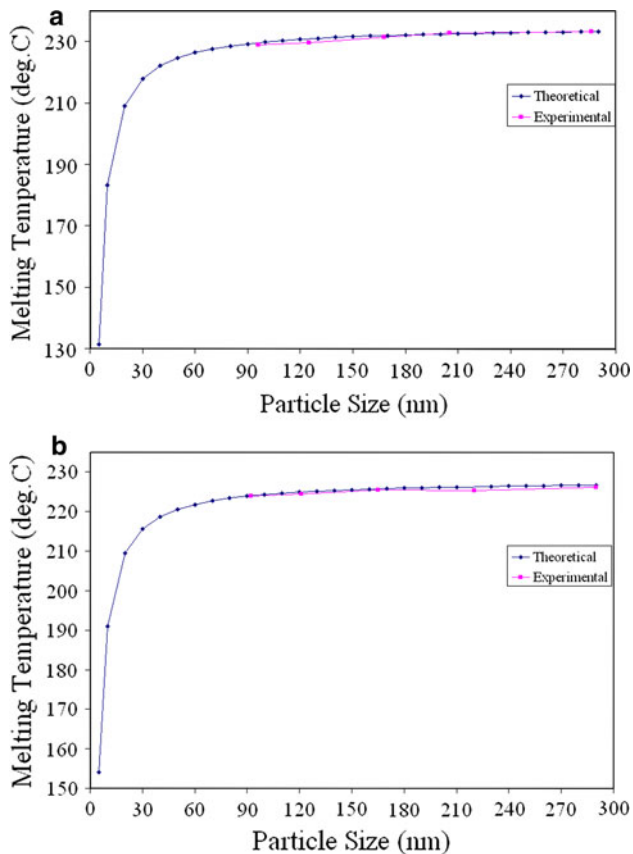
where, ΔT is the difference in melting point of bulk and nanosized material, T_m^{bulk} is the melting point of the bulk material, $T_m(r)$ is the melting point of the nanosized material, H_m^{bulk} is the heat of fusion of the bulk material, ρ_S is the solid phase density of the bulk material, ρ_L is the liquid phase density of the bulk material, σ_S is the surface tension of the solid-vapour interface, σ_L is the surface tension of the liquid-vapour interface, and r is the radius of the nanosized particles.

Table 1 show the data used in calculating the melting point depressions due to nanosize effect by using above equation. The heat of fusion for bulk solders was determined by means of DSC. The density and surface tension values for Sn-3.5Ag and Sn-0.7Cu were considered from ref [9]. The densities for both the alloys are assumed to be the same in both solid and liquid phases near melting [10].

The two curves in Fig. 4 shows melting temperatures of theoretically estimated values (continuous lines upto 5 nm sizes) and the experimental data (solid lines upto ~90 nm sizes). The calculated melting point values are in good agreement with the experimental data and most

Table 1 Data used in calculations of theoretical melting temperatures

Parameters	Sn-3.5Ag	Sn-0.7Cu
T_m^{bulk}	228 °C	235 °C
H_m^{bulk}	60.25 J/g	52.65 J/g
ρ_s	7.39 g/cm ³	7.29 g/cm ³
ρ_L	7.39 g/cm ³	7.29 g/cm ³
σ_s	512×10^{-3} J/m ²	584×10^{-3} J/m ²
σ_L	431×10^{-3} J/m ²	491×10^{-3} J/m ²

**Fig. 4** Melting temperature dependence of **a** Sn-3.5Ag and **b** Sn-0.7Cu alloys as a function of nanoparticles

interestingly, as particle sizes fall below 50 nm, the melting temperatures are drastically coming down. This ensures that further reduction in the crystallite size results in more

prominent depletion in melting temperatures. It is possible to achieve the conventional lead solder reflow temperatures around 30 nm sizes in both the alloys and a significant reduction of temperatures expected when the particle radius approaches 20 nm.

4 Conclusions

Mechanical attrition of stir cast alloys is a novel feasible approach to manufacture high quality lead-free solders for electronic products. Nanosized Sn-3.5Ag and Sn-0.7Cu lead free solder alloys were successfully synthesized and tested for their size dependent melting characteristics. A gradual transformation from sharp endothermic peaks in bulk alloys to broad low temperature peaks at reduced particle sizes from DSC measurements show a great potential to tune the melting temperatures of the alloys to the desired values depending on application domain. The theoretically calculated melting temperatures are in good agreement with the experimental data and the results reveal a significant melting point depression is possible in the given alloys when the particle radius approaches close to 20 nm. There is a high potential for the technique in manufacturing large amounts of nanoparticles with controlled shape, small size, narrow particle size distribution and nearly oxide-free composition.

References

1. Press Releases (2001) <http://www.nemi.org/PbFreePUBLIC/Alloy/PRO12400.html>
2. Lead-free Alloys-The way Forward (1999) <http://www.lead-free.org>
3. Ph. Buffat, J.P. Borel, Phys. Rev. A. **13**, 2287–2298 (1976)
4. M. Takagi, J. Phys. Soc. Jpn. **359**, 9 (1954)
5. M. Wautelet, Eur. J. Phys. **16**, 283–284 (1995)
6. K.K. Nanda et al., Eur. J. Phys. **19**, 471–472 (1998)
7. F. Ercolessi, W. Andreoni, E. Tosetti, Phys. Rev. Lett. **66**, 911–914 (1991)
8. E.A. Olson, M. Yu Efremov, M. Zhang, L.H. Allen, J. Appl. Phys. **97**, 034304 (2005)
9. A. Mulugeta, G. Selvanduray, Mater. Sci. and Engg., R. **27**, 95–114 (2000)
10. G.L. Allen, R.A. Bayels, W.W. Gile, W.A. Jesser, Thin Solid Films **144**, 297–308 (1986)